Supplementary Information

Synthesis of amorphous *Geobacter*-manganese oxide biohybrid as efficient water oxidation catalysts

Shafeer Kalathil, Krishna P. Katuri, Pascal E. Saikaly*

Division of Biological and Environmental Sciences & Engineering, Water Desalination and Reuse Center, King Abdullah University of Science and Technology, Thuwal 23955-6900, Saudi Arabia

Email: pascal.saikaly@kaust.edu.sa

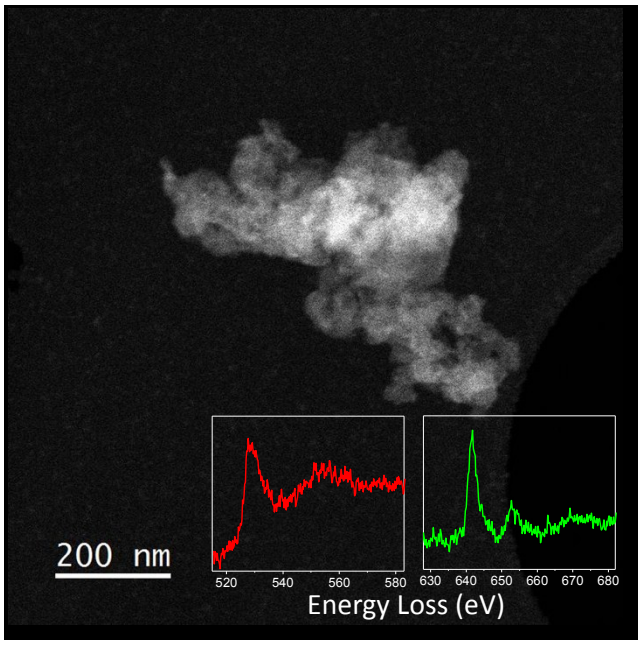

Fig. S1 Scanning transmission electron microscopy-high angle annular dark field (STEM-HAADF) image shows no Mn_2O_3 production with Δcyts cells. Lower inset shows the corresponding electron energy loss spectra (EELS).

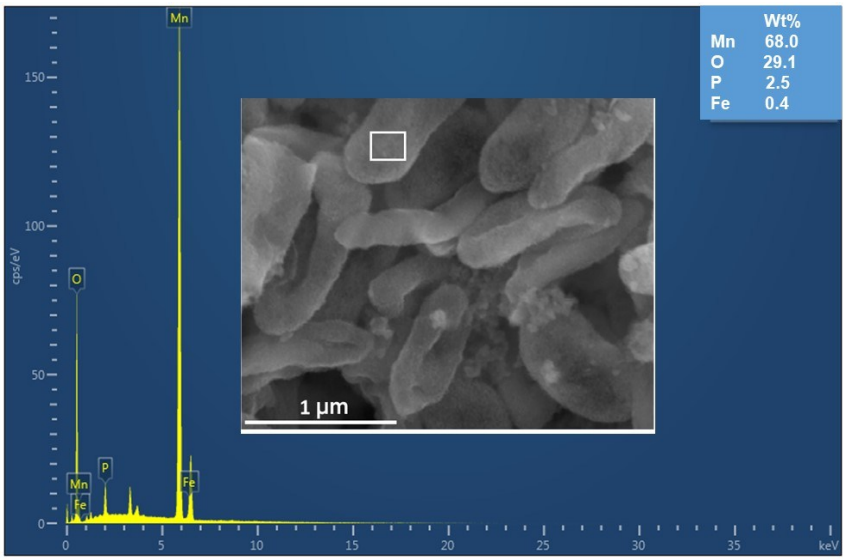

Fig. S2 SEM-EDX spectrum of *Geobacter*-Mn_2O_3 biohybrid.

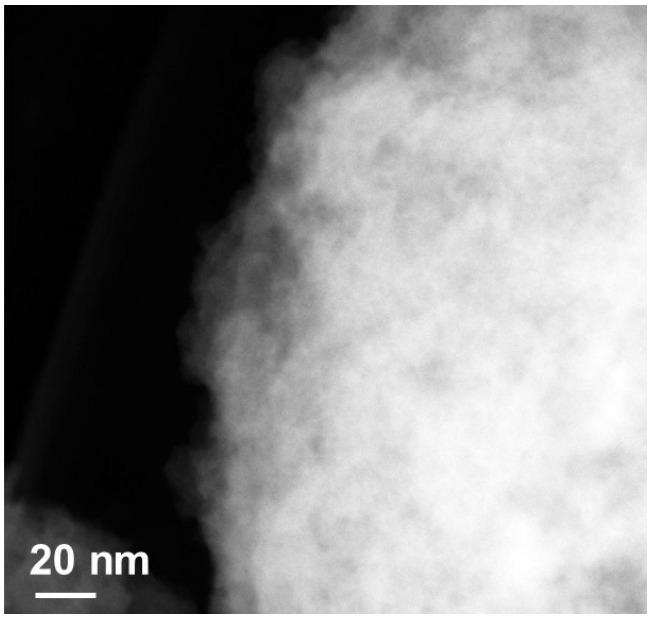

Fig. S3 HRTEM image of *Geobacter*-Mn_2O_3 biohybrid.

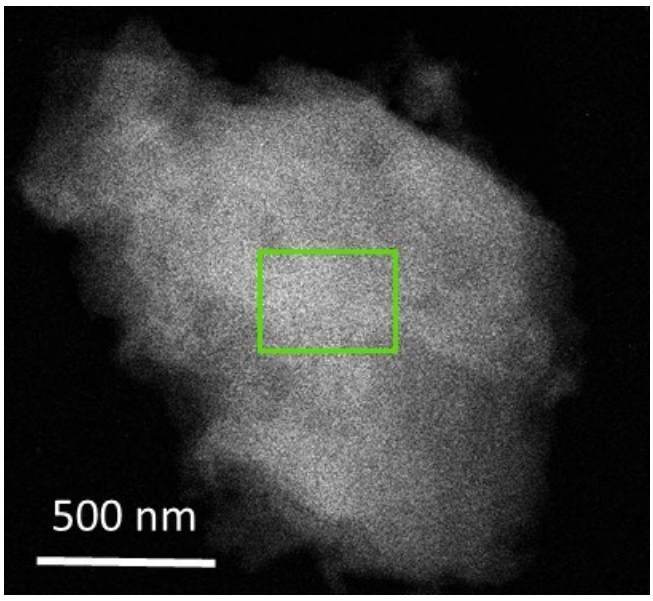

Fig. S4 STEM-HAADF image of commercial-Mn_2O_3. The green square shows the location of EELS maps obtained.

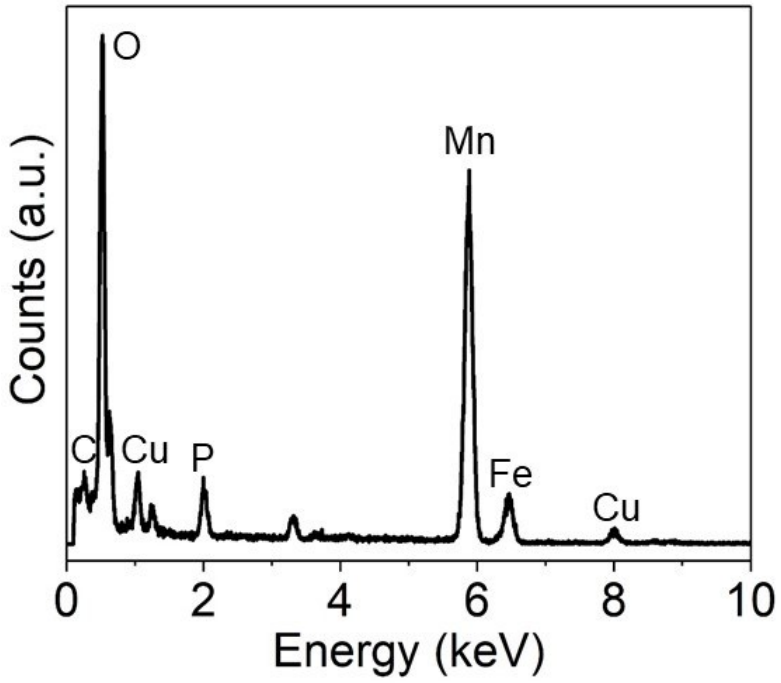

Fig. S5 TEM-EDX spectrum of *Geobacter*-Mn_2O_3 biohybrid.

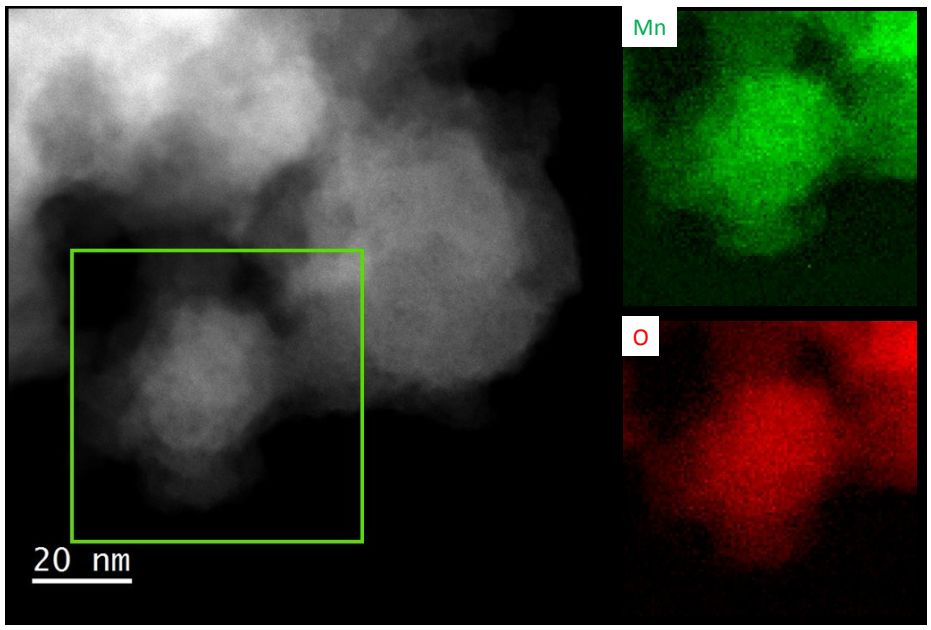

Fig. S6 STEM-HAADF image of the Mn_2O_3 nanocrystals located at the surface of *G. sulfurreducens* (left). EELS maps obtained (the green square in the left image) from Mn-L2,3 (green) and O-K (red) edges, respectively (right).

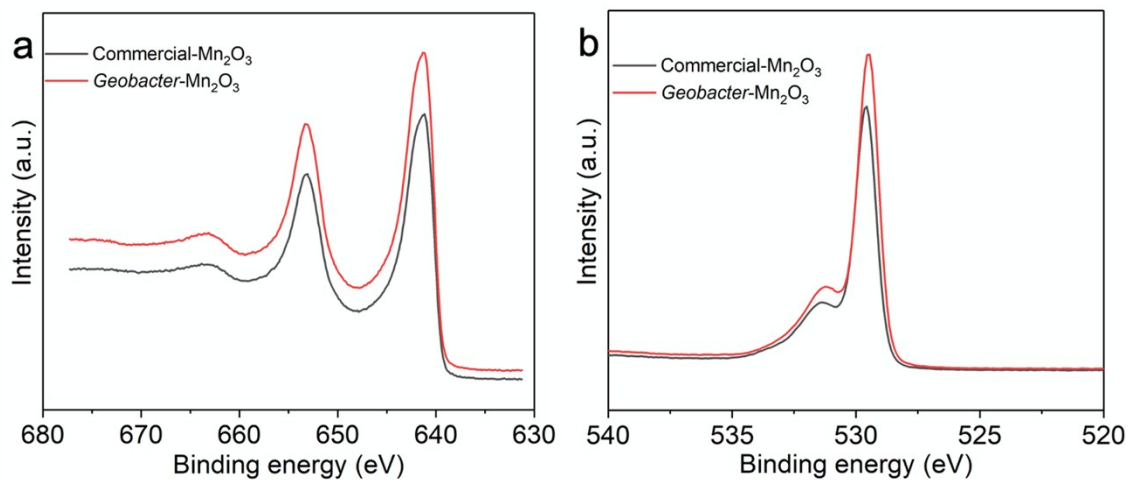

Fig. S7 XPS spectra of commercial-Mn_2O_3 and *Geobacter*-Mn_2O_3 (a) Mn 2p and (b) O1s.

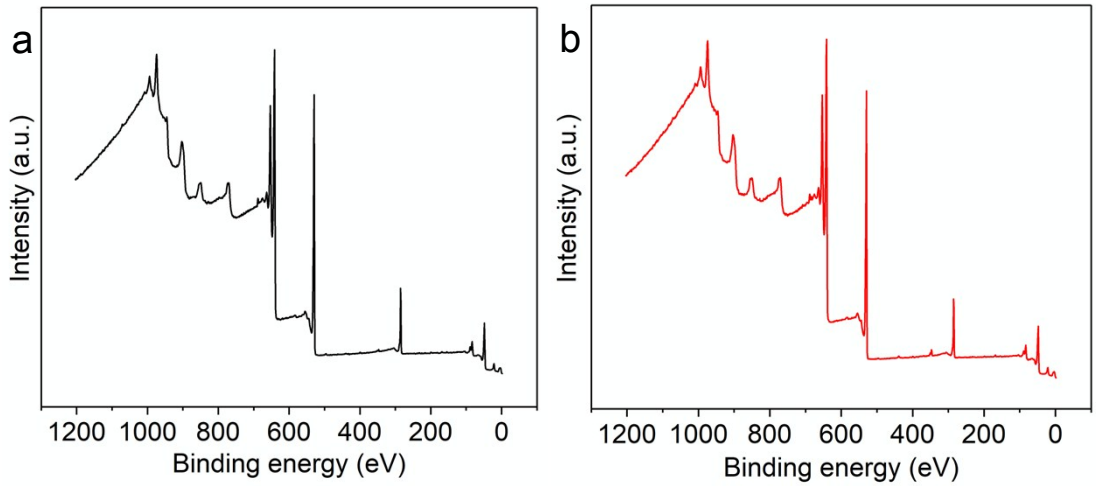

Fig. S8 XPS full scan spectra of commercial-Mn_2O_3 (a) and *Geobacter*-Mn_2O_3 (b).

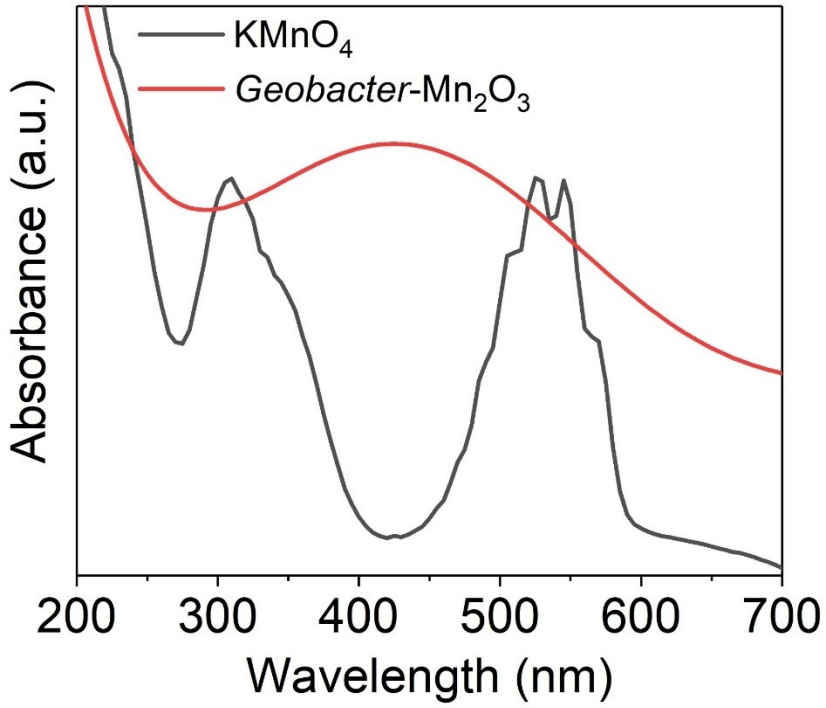

Fig. S9 UV-vis spectra of precursor ($KMnO_4$) and Geobacter-Mn_2O_3.

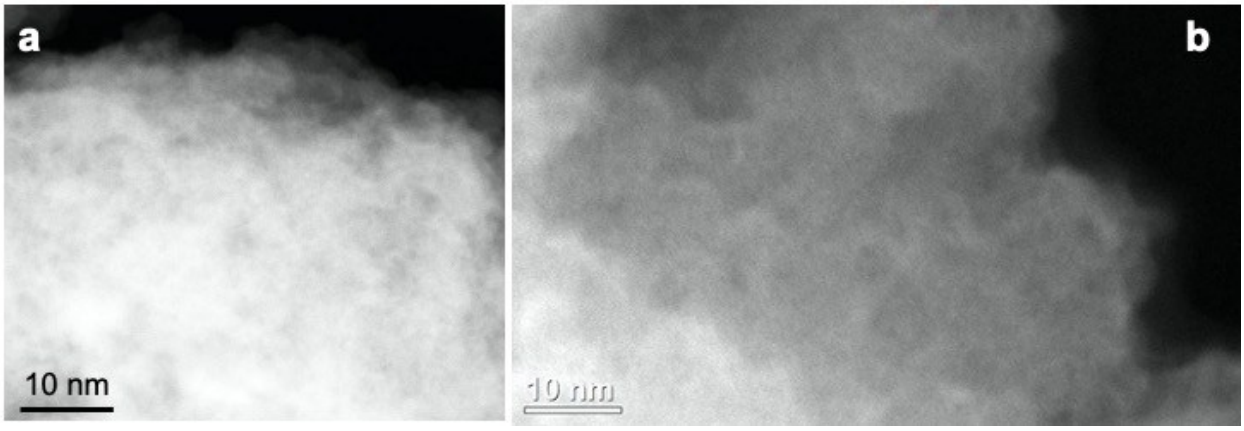

Fig. S10 HRTEM images of *Geobacter*-Mn_2O_3 biohybrid (a) before the OER stability test and (b) after the stability test.

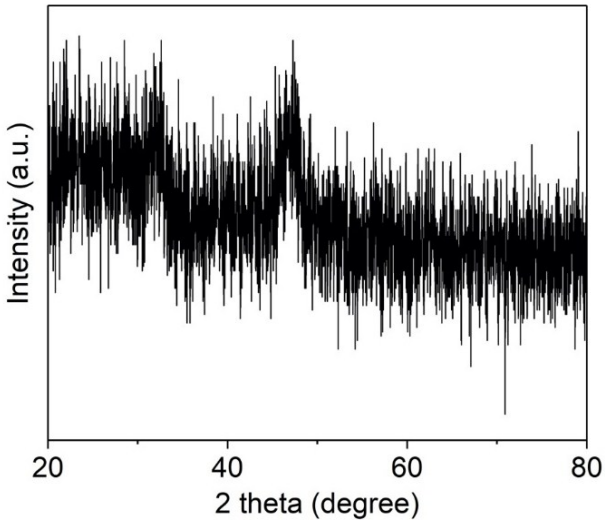

Fig. S11 XRD profile of the biohybrid after the OER stability test.

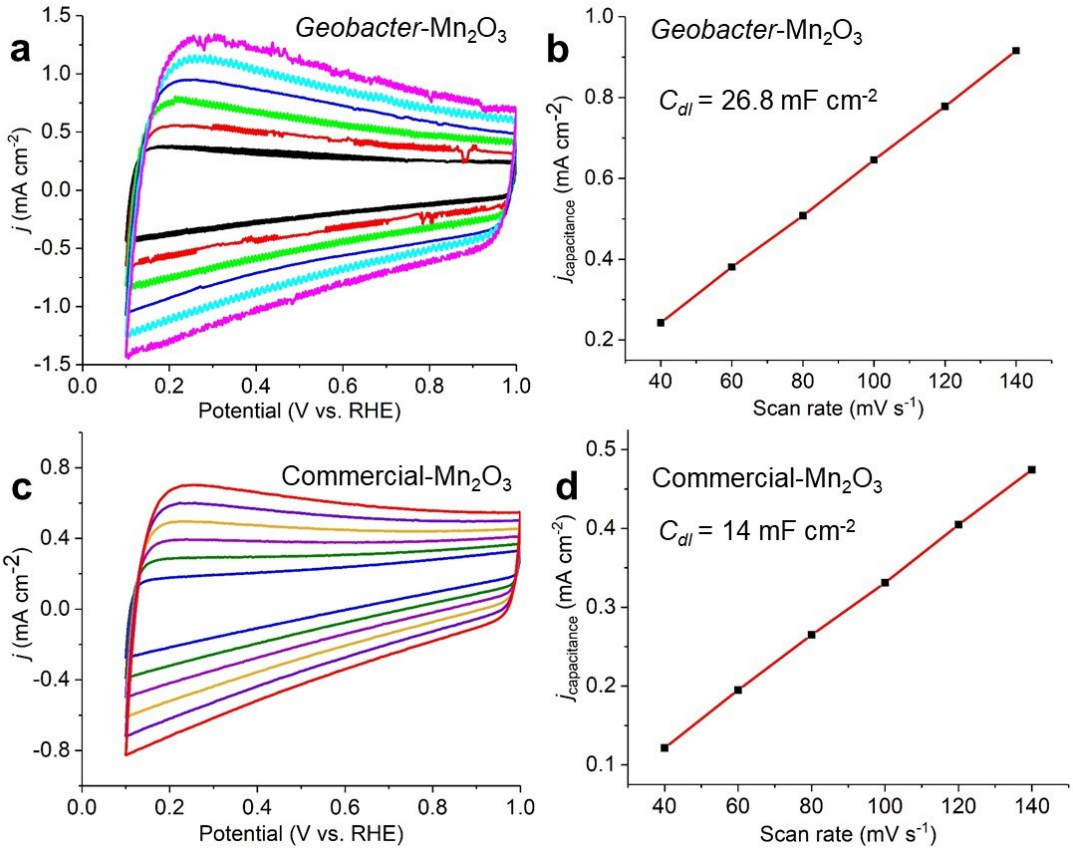

Fig. S12 Electrochemically active surface area determination. a, b Determination of double-layer capacitance over a range of scan rates for *Geobacter*-Mn_2O_3 biohybrid. c,d Determination of double-layer capacitance over a range of scan rates for commercial-Mn_2O_3.

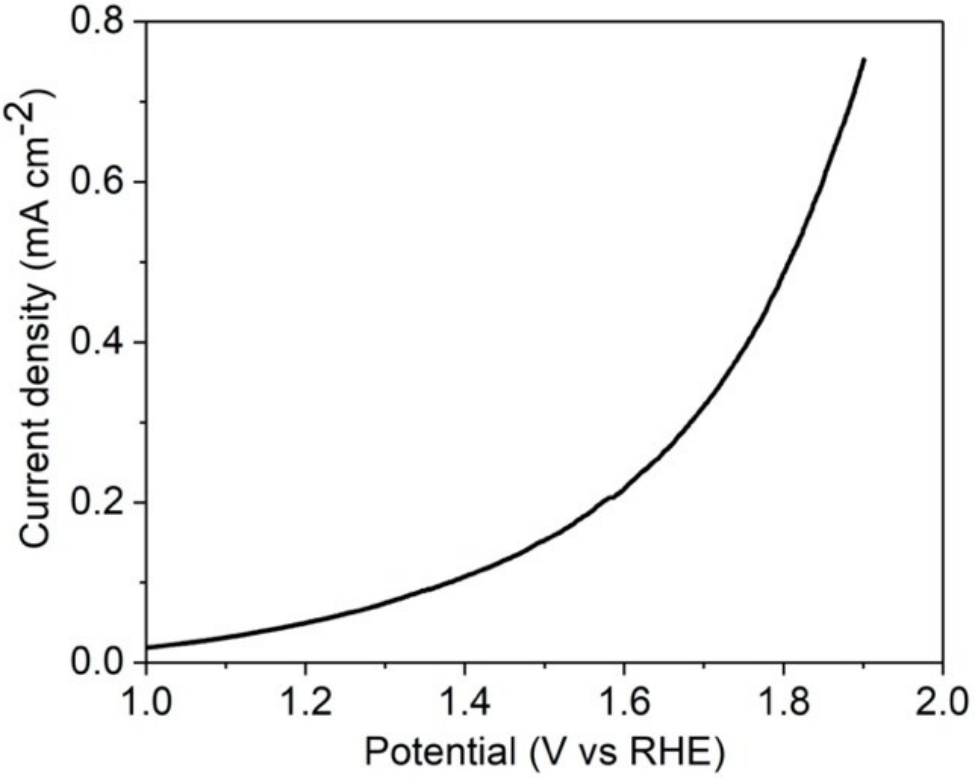

Fig. S13 OER activity of pure *G. sulfurreducens* cells.

Table S1. Comparison of the OER performance of amorphous *Geobacter*-Mn_2O_3 biohybrid with benchmark OER electrocatalysts.

catalyst	overpotential (mV) @ 10 mA cm^{-2}	Tafel (mV dec^{-1})	reference
Amorphous *Geobacter*-Mn_2O_3	290	59	This study
Commercial-IrO_2	390	112	This study
Tri-doped (O, N, and P) carbon cloth	410	83	[1]
Tri-doped graphene (N, P, F)	390	136	[2]
Ni_2P	290	59	[3]
Pt/C	450	86	[1]
IrO_2-CNT	620	83	[4]
IrO_2	350	89	[5]
N, O doped Graphene-CNT	410	141	[6]
Co/CoOx40-MC1050	429	58	[7]
NiCuCo-sulfides	340	89	[8]
Ni/Fe LDH	300	40	[9]
$CuCo_2S_4$	310	86	[10]

References

1. J. Lai, S. Li, F. Wu, M. Saqib, R. Luque and G. Xu, *Energy Environ. Sci.,* 2016, **9**, 1210.

2. J. Zhang and L. Dai, *Angew. Chem. Int. Ed.,* 2016, **55**, 13296.

3. L-A. Stern, L. Fang, F. Song and X. Hu, *Energy Environ. Sci.,* 2015, **8**, 2347.

4. K. Qu, Y. Zheng, S. Dai and S. Z. Qiao, *Nano Energy*, 2016, **19**, 373.

5. X. Li, Y. Fang, S. Zhao, J. Wu, F. Li, M. Tian, X. Long, J. Jin and J. Ma, *J. Mater. Chem. A*, 2016, 4, 13133.

6. S. Chen, J. Duan, M. Jaroniec, S-Z. Qiao*, Adv. Mater.,* 2014, **26**, 2925.

7. H. Pan, D. Wu, X. Huang, K. Xie, H. He, Z. Lu, P. Liu, J. Cheng, X. Zhao, J. Masa and X. Chen, *J. Electrochem. Soc.,* 2019, **166**, F479.

8. X. Wu, S. Li, J. Liu and M. Yu, *ACS Appl. Nano Mater.,* 2019, **2**, 4921.

9. Y. Zhu, G. Chen, Y. Zhong, Y. Chen, N. Ma, W. Zhou and Z. Shao, *Nat. Commun.,* 2018, **9**, 2326.

10. M. Chauhan, K. P. Reddy, C. S. Gopinath and S. Deka, *ACS Catal.,* 2017, **7**, 5871.